Available online at www.sciencedirect.com
ScienceDirect
Mathematics and Computers in Simulation 167 (2020) 356–371
MATHEMATICS AND COMPUTERS IN SIMULATION
www.elsevier.com/locate/matcom

Original articles

An advanced control for a PM synchronous motor drive in power degraded mode

O. Béthoux[a,*], E. Labouré[a], E. Berthelot[a], A. Kolli[b], A. De Bernardinis[b]

[a] *GeePs—Group of electrical engineering – Paris, UMR CNRS 8507 CentraleSupélec, Univ Paris-Sud, Sorbonne Universités, UPMC Univ Paris 06 3, 11 rue Joliot-Curie, Plateau de Moulon, F-91192 Gif-sur-Yvette CEDEX, France*
[b] *SATIE (UMR 8029), IFSTTAR, CNRS, ENS Cachan, CNAM, Université, Cergy-Pontoise, F-78000 Versailles, France*

Received 15 January 2018; received in revised form 31 August 2018; accepted 1 February 2019
Available online 15 February 2019

Abstract

This paper deals with a control principle designed to allow remedial strategies for Permanent Magnet Synchronous Motor (PMSM) drives. The scope of the paper is focused on three-phase machines and it aims to present a simple and easy to tune control scheme for the system while it operates in degraded mode, namely when only two out of the three phases are operational. Compared to existing control strategy dedicated to degraded mode, this work proposes an innovative one using new reference frames. Based on two innovative transformations applied respectively to the currents and the voltages of the system, the proposed control scheme allows, in degraded mode, the decoupling control of the states of the system and leads to continuous controller references during system steady states. These properties lead to a very straightforward control scheme based on independent PI controllers and to high static and dynamic performances. The parameters setting of the controller is quite simple whatever the degree of magnetic coupling between the two remaining motor phases. A laboratory test bench has been built to establish a proof of concept of the suggested remedial strategy. It is based on a three-phase open-end-winding permanent magnet machine fed with a power inverter made of three full H-bridge. This experimental setup enables to validate the main operations of the ac motor drive under degraded mode operation: torque control, speed change. Switching between healthy mode and faulty mode is also performed successfully using this setup.

Keywords: Fault-tolerant control; Control scheme; Permanent-magnet synchronous motor (PMSM) drive; Phase loss; Remedial strategy

1. Introduction

Electric motor drives are often used for key functionalities which are mission critical and cannot tolerate any unexpected periods of downtime due to a failure. Examples include many manufacturing processes [13,23] and transport applications [31]. For instance power-assisted steering of a ground vehicle [3,26] or the actuators of the control surfaces of a plane [33] are key examples. Some of these applications call for demanding specifications regarding high power density and high efficiency. In such cases, the best choice is often a permanent magnet synchronous machine [29]. This constraint is frequently associated with embedded systems and usually coincides with a requirement for a high level of availability and reliability.

* Corresponding author.
E-mail address: olivier.bethoux@centralesupelec.fr (O. Béthoux).

https://doi.org/10.1016/j.matcom.2019.02.001

Several strategies can be successful in designing a fault-tolerant motor drive architecture. A first example is increasing the number of converters either in parallel [34] or in series [25] as well as the number of power switches using multicellular converters [19]. The second method that has been explored is increasing the number of machines [21]. The third is using multiphase machines, generally with an odd number of phases [22,32]. These three methods are usually applied in high power applications or products for which cost is not a key feature. However, the last solution can also be used in low cost applications whilst permitting fault tolerant operation. For this purpose, the lowest multiphase machine ($n = 3$) is the basic 3-phase motor. Two ways can be used to achieve a fault-tolerant architecture: (1) using a 4-leg inverter and connecting the ac machine neutral point to the fourth leg [6,7], (2) using a 3-phase open-end-winding ac machine supplied by a power inverter made of three full H-bridge [15,18]. For example, the latter solution is proposed in the car industry. It is covered by several patents owned by VALEO [8,10–12]; the overall system allows achieving the three key power function of an electric vehicle, namely traction [28], fast and slow charging [17], and grid assistance [27]. For this reason, the work covered here aims at designing a proper control scheme, both simple and efficient to achieve the 2-phase operation mode of such a 3-phase synchronous machine.

Switching from a 3-phase to a 2-phase operation entails a structural change. In the 4-leg inverter case, the phase currents sum is no longer equal to zero, in the open-winding case, the system dimension decreases from three to two. To address this issue, S. Bolognani et al. computed the optimal sinusoidal current reference for post fault operation [7]. They implemented this strategy using a 4-leg inverter [6]. Their suggested fault-mode operation control scheme is based on the Park fictitious machine. This leads to fictitious voltages with additional sinusoidal terms. As PI controllers are not able to manage them properly, the control effectiveness is essentially based on the cancellation of such terms. This indicates that this control scheme is primarily defined by the precise knowledge of the motor parameters. Within the specific framework of a fully decoupled synchronous machine, F. Baudart et al. calculate the optimal current references for any number of motor phases [5]. In this specific case the current references track does not present any particular difficulties since the system is structurally decoupled.

The aim of this article is to propose a unified approach enabling to design a control scheme for achieving the real-time control of a 3-phase synchronous machine in 2-phase faulty mode. The desired key points are: (1) simple to implement control scheme, (2) easy tuning of controllers parameters, (3) constant control values delivered by the controllers in steady state, namely whilst torque and speed are constant. The present work gives a clear insight of the theoretical basis related to the proposed approach and goes on to its proof-of-concept in laboratory test bench trials.

This paper is organized as follows. The second section presents the fictitious machine related to the aforementioned specifications. This leads to present the innovative transform matrices applied to the electric values (e.g., currents and voltages). These transformations describe the link between real and fictitious machines whose model will be presented in this part. The third section then considers the appropriate control scheme of the two remaining phase currents and explains the controller parameter setting method. The fourth section focuses on the experimental validation of the suggested transformation concept and the related control scheme. The developed experimental setup is described and trial results are presented and commented. This fully validates the ability of the control scheme to maintain motor drive key functions during the application of the remedial strategy as well as showing that switching from normal to faulty mode can be realized safely. Finally, the last section draws conclusion and perspectives for future work.

2. Innovative transformations and fictitious machine

The present section addresses the control of only two phase currents of a 3-phase synchronous machine. For clarity all notations are summarized in Table 1. An innovative set of transformations is proposed in order to tackle this issue effectively. The aim is to design a fictitious machine (Fig. 1) which

(1) Produces the same magneto-motive force m.m.f. ε than the real machine but by the means of two decoupled windings (these are being therefore orthogonal) fed by the fictitious current $\begin{bmatrix} i_\gamma & i_\delta \end{bmatrix}^T$;
(2) Is driven by the fictitious voltage $\begin{bmatrix} v_\gamma & v_\delta \end{bmatrix}^T$ enabling instantaneous power invariance;
(3) Is supplied by constant variables during steady state (specifically while torque and rotational speed are constant).

Table 1
Nomenclature of the terms and symbols used in the document.

Symbol	Parameter
$[i_a \ i_b]$	Real 3-phase machine winding currents in degraded mode
$[v_a \ v_b]$	Real 3-phase machine winding voltages in degraded mode
L_a and L_b	Self-inductances of the two remaining windings
M_{ab}	Mutual inductance of the two remaining windings
R	Resistance of each winding
θ_e	Rotor electrical angular position
ω_e	Electric angular frequency
Ω	Mechanic angular frequency
ε	Magneto-motive force induced by the stator currents
x	Considered angular position in the machine air gap
N_s	Number of turns of the machine windings
T_i	Two remaining currents transformation
T_v	Two remaining voltages transformation
θ_{fr}	Relative angular position of the fictitious frame to that of the rotor
$[i_\gamma \ i_\delta]$	Fictitious 3-phase machine winding currents in degraded mode
$[v_\gamma \ v_\delta]$	Fictitious 3-phase machine winding voltages in degraded mode
K_{SM}	Speed constant of the fictitious machine
$[i_{\gamma,ref} \ i_{\delta,ref}]$	Fictitious current references
K_p	Coefficient for the proportional term of the PI controller
ω_I	Coefficient for the integral term of the PI controller
H_k	Transfer function of the current closed-loop
ω_0	Desired bandwidth of the current closed-loop
m	Damping factor of the current closed-loop
V_{DC}	DC voltage value of the power inverter supply
F_{SW}	Switching frequency of the power inverter
T_S	Sampling time of the digital controller
T_{ref}	Machine torque reference

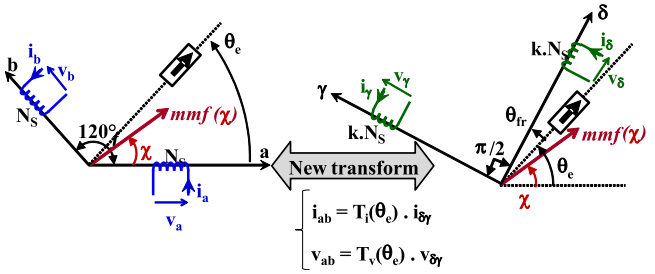

Fig. 1. Real and fictitious machines associated to innovative set of transformations.

Note that it is considered here in an arbitrary manner that the faulty phase is the c-phase.

To meet these three requirements, a set of two transformations T_i and T_v has to be defined. The first function is applied to the current and the second to the voltage. Obviously, the two mentioned functions depend on the rotor electrical angular position defined by $\theta_e(t)$.

$$\begin{bmatrix} i_a \\ i_b \end{bmatrix} = T_i(\theta_e) \begin{bmatrix} i_\delta \\ i_\gamma \end{bmatrix} \tag{1}$$

$$\begin{bmatrix} v_a \\ v_b \end{bmatrix} = T_v(\theta_e) \begin{bmatrix} v_\delta \\ v_\gamma \end{bmatrix} \tag{2}$$

with $\begin{bmatrix} i_a & i_b \end{bmatrix}^T$ and $\begin{bmatrix} v_a & v_b \end{bmatrix}^T$, the real machine current and voltage, respectively.

The θ_{fr} parameter described in Fig. 1 is a parameter which should be chosen to give the most convenient position of the new rotating frame. Likewise, the k parameter defines the voltage ratio between fictitious and real winding.

Based on the requirements, the three following subsections define the suggested transformation set. The fourth subsection derives the control-oriented model of the fictitious machine.

2.1. Power invariance

To ensure that the two machines are equivalent, it is mandatory to ensure that the instantaneous power consumption of each machine are equal, as follows:

$$\begin{bmatrix} v_a \\ v_b \end{bmatrix}^T \begin{bmatrix} i_a \\ i_b \end{bmatrix} = \begin{bmatrix} v_\delta \\ v_\gamma \end{bmatrix}^T T_v(\theta_e)^T T_i(\theta_e) \begin{bmatrix} i_\delta \\ i_\gamma \end{bmatrix} = \begin{bmatrix} v_\delta \\ v_\gamma \end{bmatrix}^T \begin{bmatrix} i_\delta \\ i_\gamma \end{bmatrix} \tag{3}$$

This mathematical equality implies the following relation between the two transfer matrix T_i and T_v:

$$T_v(\theta_e)^T T_i(\theta_e) = Id \tag{4}$$

2.2. Remaining currents transformation

The m.m.f. ε_{real} of the real machine is expressed as a function of real currents. Noting x the angular position in the machine air gap, ε_{real} can be computed as:

$$\varepsilon_{real} = AN_S \begin{bmatrix} \cos(x) & \cos(x - 2\pi/3) \end{bmatrix} \begin{bmatrix} i_a \\ i_b \end{bmatrix} \tag{5}$$

with N_S the number of turns of the machine windings and A a machine geometry-dependent parameter.

To simplify motor drive control, it is useful to separate the two current components. This means, from a mathematical point of view, that the transformation must achieve the diagonalization of the inductance matrix $L_{ab}(\theta_e)$ defined by:

$$L_{ab}(\theta_e) = \begin{bmatrix} L_a(\theta_e) & M_{ab}(\theta_e) \\ M_{ab}(\theta_e) & L_b(\theta_e) \end{bmatrix} \tag{6}$$

with L_a and L_b the self-inductances of the two remaining windings and M_{ab} their mutual inductance.

This first requirement involves the choice of two orthogonal fictitious winding, as depicted in Fig. 1. Equally, the requirement of having constant currents at steady state implies that the fictitious windings rotate synchronously with the rotor.

Using these preliminary findings, the second m.m.f. ε_{fict} is directly expressed in the new $\delta\gamma$ frame.

$$\varepsilon_{fict} = AkN_S \left[\cos\left(x - \theta_e - \theta_{fr}\right) \cos\left(x - \theta_e - \theta_{fr} - \frac{\pi}{2}\right) \right] \begin{bmatrix} i_\delta \\ i_\gamma \end{bmatrix} \tag{7}$$

The trigonometric identities help to simplify this expression:

$$\varepsilon_{fict} = A.k.N_S. \begin{bmatrix} f_1(x) & f_2(x) \end{bmatrix}. \begin{bmatrix} i_\delta \\ i_\gamma \end{bmatrix} \tag{8}$$

with f_1 and f_2 two functions of angle x and angle $\theta_e(t)$:

$$\begin{cases} f_1(x) = \cos(x) \,.\, \cos\left(\theta_e + \theta_{fr}\right) + \sin(x) \,.\, \sin\left(\theta_e + \theta_{fr}\right) \\ f_2(x) = -\cos(x) \,.\, \sin\left(\theta_e + \theta_{fr}\right) + \sin(x) \,.\, \cos\left(\theta_e + \theta_{fr}\right) \end{cases} \tag{9}$$

At a general level, the transformation matrix T_i is characterized by four entries (a, b, c and d):

$$T_i(\theta_e) = \begin{bmatrix} a & b \\ c & d \end{bmatrix} \tag{10}$$

Using T_i definition (1), the m.m.f. of the real machine ε_{real} is expressed as a function of the fictitious currents:

$$\varepsilon_{real} = AN_S \begin{bmatrix} \cos(x) & \cos(x - 2\pi/3) \end{bmatrix} \begin{bmatrix} a & b \\ c & d \end{bmatrix} \begin{bmatrix} i_\delta \\ i_\gamma \end{bmatrix} \tag{11}$$

Using trigonometric identities yields the final expression:

$$\varepsilon_{real} = AN_S \begin{bmatrix} g_1(x) & g_2(x) \end{bmatrix} \begin{bmatrix} i_\delta \\ i_\gamma \end{bmatrix} \tag{12}$$

with g_1 and g_2 determined by angle x and angle $\theta_e\,(t)$:

$$\begin{cases} g_1\,(x) = \cos\,(x)\,.\,(a - c/2) + \sin\,(x)\,.\,\left(c.\sqrt{3}/2\right) \\ g_2\,(x) = \cos\,(x)\,.\,(b - d/2) + \sin\,(x)\,.\,\left(d.\sqrt{3}/2\right) \end{cases} \tag{13}$$

The identification of the four relevant parameters is obtained by equating both expressions of m.m.f. (8) and (12) whatever the position in the air gap ($0 \leq x \leq 2\pi$) and the two components of the fictitious current. This comparison leads to a system of four nonlinear equations involving the four listed parameters: a, b, c and d.

$$\begin{cases} a - c/2 = \mathrm{k}\cos\left(\theta_e + \theta_{fr}\right) \\ c.\sqrt{3}/2 = \mathrm{k}\sin\left(\theta_e + \theta_{fr}\right) \\ b - d/2 = -\mathrm{k}\sin\left(\theta_e + \theta_{fr}\right) \\ d.\sqrt{3}/2 = \mathrm{k}\cos\left(\theta_e + \theta_{fr}\right) \end{cases} \tag{14}$$

Deciding arbitrarily that the real machine and the fictitious one have the same number of turns ($k = 1$), (14) allows to derive the current transformation matrix:

$$T_i\,(\theta_e) = \frac{2}{\sqrt{3}}\begin{bmatrix} \cos\left(\theta_e + \theta_{fr} - \pi/6\right) & -\sin\left(\theta_e + \theta_{fr} - \pi/6\right) \\ \sin\left(\theta_e + \theta_{fr}\right) & \cos\left(\theta_e + \theta_{fr}\right) \end{bmatrix} \tag{15}$$

Unlike the Concordia or Park transformations, it is important to note that this matrix is non-orthogonal. Indeed the inverse matrix of the matrix T_i is:

$$T_i^{-1} = \begin{bmatrix} \cos\left(\theta_e + \theta_{fr}\right) & \sin\left(\theta_e + \theta_{fr} - \pi/6\right) \\ -\sin\left(\theta_e + \theta_{fr}\right) & \cos\left(\theta_e + \theta_{fr} - \pi/6\right) \end{bmatrix} \neq T_i^T \tag{16}$$

This is because instantaneous power invariance does not impose this constraint for a 3-phase ac machine when working only with two phases as shown in (4).

The θ_{fr} parameter is chosen by allocating a specific role to each fictitious winding. For instance, a wise choice consists in using i_δ current for adjusting the machine magnetization and i_γ for controlling the electromagnetic torque T_{em}. This is obtained by imposing θ_{fr} equal to zero. Doing so and adopting $i_{\delta\gamma}^T = \left[0 \quad T_{em}/\left(K_{SM}.\sqrt{2}\right)\right]^T$ for the fictitious currents, the real currents $\left[i_a \quad i_b\right]^T$ are calculated from (1) and (16).

$$\begin{bmatrix} i_a \\ i_b \end{bmatrix} = -\frac{T_{em}}{K_{SM}.\sqrt{3}}\sqrt{2}\begin{bmatrix} \sin\,(\theta_e - \pi/6) \\ \sin\,(\theta_e - \pi/2) \end{bmatrix} \tag{17}$$

where K_{SM} is the motor electromotive force constant defined by $K_{SM} = E/\Omega$.

Obviously (17) is similar to optimal sinusoidal current reference determined by [7]. Hence the first transformation T_i is well defined and the self-control current reference is also found in this unified approach. The second step is to compute the voltage allowing to achieve these currents. To do so, the next subsection exhibits the voltage transformation T_v.

2.3. Voltage transformation

As mentioned before, ensuring the power invariance imposes a constraint on voltage transformation matrix. Within the $\delta\gamma$ frame with $\varphi = 0$, and using (4), T_v matrix is expressed as:

$$T_v = \left(T_i^{-1}\right)^T = \begin{bmatrix} \cos\,(\theta_e) & -\sin\,(\theta_e) \\ \sin\,(\theta_e - \pi/6) & \cos\,(\theta_e - \pi/6) \end{bmatrix} \tag{18}$$

Considering the case of a sinusoidal back electromotive force $e_{ab} = [e_a \; e_b]^T$

$$\begin{bmatrix} e_a \\ e_b \end{bmatrix} = -K_{SM}\sqrt{2}\left(\frac{1}{p}\cdot\frac{d\theta_e}{dt}\right)\begin{bmatrix} \sin\,(\theta_e) \\ \sin\,(\theta_e - 2\pi/3) \end{bmatrix} \tag{19}$$

The fictitious expression of back electromotive force $e_{\delta\gamma} = \left[e_\delta \; e_\gamma\right]^T$ can then be derived:

$$\begin{bmatrix} e_\delta \\ e_\gamma \end{bmatrix} = K_{SM}\cdot\sqrt{2}\cdot\left(\frac{1}{p}\cdot\frac{d\theta_e}{dt}\right)\cdot\begin{bmatrix} 0 \\ 1 \end{bmatrix} \tag{20}$$

This is obviously a constant vector with a zero δ component and a γ component with the same magnitude than the real back electromotive force. The result is consistent with the expectations on this transformation. The next stage therefore consists in deriving the control-oriented model of the fictitious machine.

2.4. Fictitious machine model

In degraded mode operation i.e. with two out of three windings operating the real machine is described by a 2-dimensional equation system:

$$\begin{bmatrix} v_a \\ v_b \end{bmatrix} = L_{ab} \frac{d}{dt} \begin{bmatrix} i_a \\ i_b \end{bmatrix} + R \begin{bmatrix} i_a \\ i_b \end{bmatrix} + \begin{bmatrix} e_a \\ e_b \end{bmatrix} \tag{21}$$

Using the two suggested transformation matrix T_i and T_v yields the fictitious machine model:

$$\begin{bmatrix} v_\delta \\ v_\gamma \end{bmatrix} = T_v^{-1} L_{ab} T_i \frac{d}{dt} \begin{bmatrix} i_\delta \\ i_\gamma \end{bmatrix} + T_v^{-1} L_{ab} \omega_e \frac{dT_i}{d\theta_e} \begin{bmatrix} i_\delta \\ i_\gamma \end{bmatrix} + R T_v^{-1} T_i \begin{bmatrix} i_\delta \\ i_\gamma \end{bmatrix} + \begin{bmatrix} e_\delta \\ e_\gamma \end{bmatrix} \tag{22}$$

where $\omega_e = d\theta_e/dt$ is the rotor electrical angular frequency.

As explained above, the last term is the back electromotive force defined in the previous paragraph. The penultimate term refers to the ohmic losses. Estimating the matrix product $T_v^{-1} T_i$ shows that this expression re-introduces a coupling between δ and γ channels. However, the fictitious ohmic voltage can be easily canceled using feed-forward terms based on current measurement and rotor angular position.

$$T_v^{-1} T_i = \frac{2}{3} \begin{bmatrix} 2\left(\sin^2(\theta_e) + \sin^2(\theta_e + \pi/3)\right) & \cos(2\theta_e + \pi/6) + \sin(2\theta_e) \\ \cos(2\theta_e + \pi/6) + \sin(2\theta_e) & 2\left(\cos^2(\theta_e) + \cos^2(\theta_e + \pi/3)\right) \end{bmatrix} \tag{23}$$

The first two terms require the knowledge of the motor inductance matrix $L_{ab}(\theta_e)$. For example, in the case of a non-salient pole rotor, the three characteristic parameters are constant. In particular, with respect to a well-coupled stator windings, the mutual inductance M depends on the winding self-inductance $L = L_a = L_b$ and is expressed as:

$$M = -L/2 \tag{24}$$

Consequently the fictitious inductance matrix $L_{\delta\gamma}$ is diagonal and has constant entries:

$$L_{\delta\gamma} = T_v(\theta_e)^{-1} L_{ab} T_i(\theta_e) = \begin{bmatrix} L & 0 \\ 0 & L \end{bmatrix} \tag{25}$$

The second term, which is proportional to rotor speed Ω and can be hence likened to a back electromotive force, is characterized by an anti-diagonal matrix with constant parameters:

$$L_{ab} \omega_e T_v(\theta_e)^{-1} . \frac{dT_i(\theta_e)}{d\theta_e} = \begin{bmatrix} 0 & -L \\ +L & 0 \end{bmatrix} . \omega_e \tag{26}$$

Finally, the model of a non-salient pole synchronous machine is fully consistent with the initial objectives. Indeed the last three terms of the related fictitious model can be offset by feedforward technique:

$$\begin{bmatrix} v_\delta \\ v_\gamma \end{bmatrix} = \begin{bmatrix} L & 0 \\ 0 & L \end{bmatrix} \frac{d}{dt} \begin{bmatrix} i_\delta \\ i_\gamma \end{bmatrix} + \begin{bmatrix} 0 & -L \\ +L & 0 \end{bmatrix} \omega_e \begin{bmatrix} i_\delta \\ i_\gamma \end{bmatrix} + R_{\delta\gamma} \begin{bmatrix} i_\delta \\ i_\gamma \end{bmatrix} + K_{SM} \Omega \sqrt{2} \begin{bmatrix} 0 \\ 1 \end{bmatrix} \tag{27}$$

3. Control scheme in degraded operation mode

The proposed fictitious machine related to the suggested transformation set is made of two orthogonal winding. The i_δ current in the first winding permits the adjustment of the air gap magnetic field whereas the i_γ current allows the control of the electromagnetic torque. Control variables are the two components of $\begin{bmatrix} v_\gamma & v_\delta \end{bmatrix}^T$ i.e., the voltages at the terminals of each motor winding. The latter are set up by a voltage inverter powered by a DC bus. To ensure a

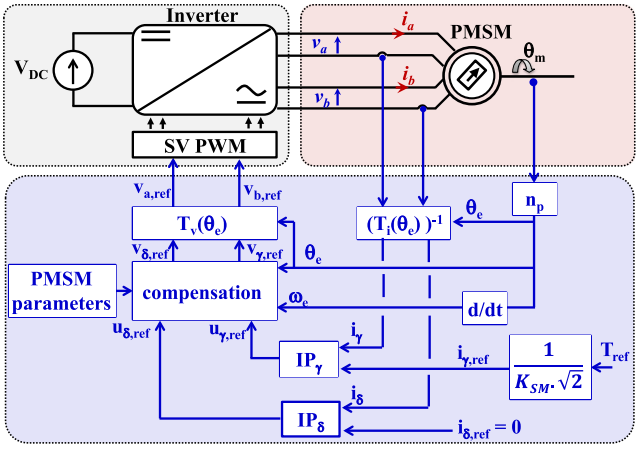

Fig. 2. Control scheme of the synchronous machine in remedial strategy.

definite decoupling of the two fictitious windings, the control scheme must simply offset the coupling terms which means providing the three feed-forward compensation terms considered in the previous paragraph (Fig. 2). By doing so the fictitious machine is simply described by a set of two independent first order linear differential equations.

$$\begin{bmatrix} u_\delta \\ u_\gamma \end{bmatrix} = \begin{bmatrix} L & 0 \\ 0 & L \end{bmatrix} \frac{d}{dt} \begin{bmatrix} i_\delta \\ i_\gamma \end{bmatrix} \tag{28}$$

where $\begin{bmatrix} u_\gamma & u_\delta \end{bmatrix}^t$ is the new control command of the decoupled fictitious machine:

$$\begin{bmatrix} v_\delta \\ v_\gamma \end{bmatrix} = \begin{bmatrix} u_\delta \\ u_\gamma \end{bmatrix} + \begin{bmatrix} 0 & -L \\ +L & 0 \end{bmatrix} \omega_e \begin{bmatrix} i_\delta \\ i_\gamma \end{bmatrix} + R_{\delta\gamma} \begin{bmatrix} i_\delta \\ i_\gamma \end{bmatrix} + K_{SM}\,\Omega\sqrt{2} \begin{bmatrix} 0 \\ 1 \end{bmatrix} \tag{29}$$

3.1. Control design

The controller parameters can be adjusted by classic control techniques such as Bode loop shaping or the root locus method [4]. Note that both subsystems have the same first-order dynamic behavior. Hence the decoupled system can be successfully controlled by two IP controllers with similar parameters. Using Laplace domain they are described by the following relations:

$$\begin{cases} u_\delta = K_P \left[-i_\delta + \left(i_{\delta,ref} - i_\delta \right) \omega_I / s \right] \\ u_\gamma = K_P \left[-i_\gamma + \left(i_{\gamma,ref} - i_\gamma \right) \omega_I / s \right] \end{cases} \tag{30}$$

The transfer function $H_k\,(s)$ between each current reference and the related current is a second-order lowpass filter whose parameters are the damping ratio m and the natural frequency ω_0:

$$\begin{aligned} H_k\,(s) &= \frac{i_k\,(s)}{i_{k,ref}\,(s)} \\ &= \frac{1}{1 + s/\omega_I + s^2/\left(K_P \omega_I / L\right)} \\ &= \frac{1}{1 + 2ms/\omega_0 + s^2/\omega_0^2} \end{aligned} \tag{31}$$

To avoid current overshoot, the desired damping ratio is settled to $m = 1$. The dynamic response of the control loop is tuned to get a closed-loop time response of about ten to twenty times the switching periods leading to $F_0 = F_{SW}/20 = 1$ kHz. These considerations induce the following parameters adjustment:

$$\omega_I = \omega_0/2m = 3.15 \text{ krad s}^{-1} \tag{32}$$

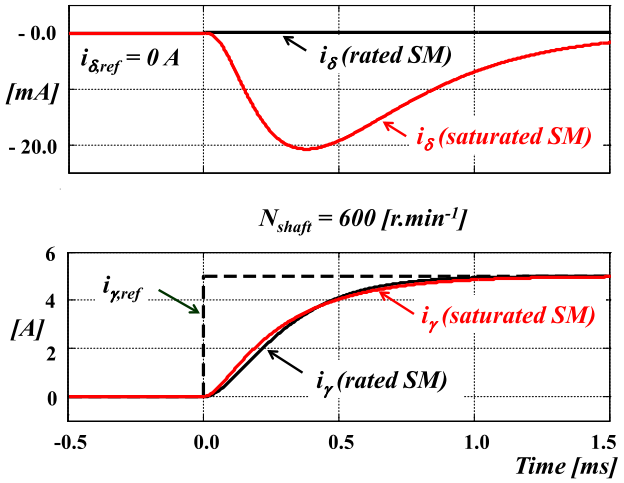

Fig. 3. Simulation of torque transient under fault operation mode: $N = 600$ r min^{-1}, $I_{\delta,ref} = 0$ A and $I_{\gamma,ref} = 0$ A $\rightarrow$ 5 A.

$$K_P = 2mL\omega_0 = 163.4 \text{ V A}^{-1} \tag{33}$$

Additionally, an anti-windup compensator [14] acts on the integral term while the demanded inverter output voltage is saturated by the DC bus supply; it may occur following a large current reference change.

3.2. Control strategy sensitivity analysis

It is critical to know in what manner and to what extent the performance of the suggested method is sensitive to the change in the motor parameters. Indeed, they could evolve over time due to internal machine temperature change or large stator current value.

Internal machine temperature may modify the B–H magnet characteristic, hence decreasing the emf while the temperature increases. As stated before, it is important to underline that the emf feedforward term is a constant. Hence an imprecise emf value does not affect the drive performance as the controller integral term can easily offset it. This also applies to the slow changes due to temperature fluctuations.

It is also necessary to consider a decrease in the inductance value due to machine magnetic saturation whilst the motor operates at high current. As previously, the IP controller can counterbalance the imprecise inductive voltage compensation in steady state mode. It should also be stressed that the dynamic decoupling is no longer ideal. However the IP controller can successfully reject this disturbance. Indeed the transfer function between the γ-current reference and the δ-current is a fourth-order bandwidth filter with high attenuation even at the resonant frequency. Fig. 3 shows a simulation which proves that a 5 A γ-reference value step leads to a negligible 11 mA δ-current overshoot in the event of an inductance decrease of 50 %. Moreover, the γ-current response has no overshoot since an inductance decrease induces an increase of the close-loop damping ratio. The response time is slightly affected by this change because the natural frequency of the closed loop is increased by this change.

3.3. Power inverter and related PWM

The suggested control strategy is a generic approach that can be applied to any voltage inverter feeding the two remaining phases of a faulty 3-phase motor. More specifically two alternative candidates [20] are:

- The 3 H-bridge inverter where each H-bridge drives a motor phase (Fig. 4);
- The 4-leg inverter whose additional leg is connected to the motor neutral point and only works in case of failure.

In the first case (Fig. 4), each phase is managed separately. Consequently the PWM scheme to be used is the basic H-bridge PWM method which produces a 3-level output voltage.

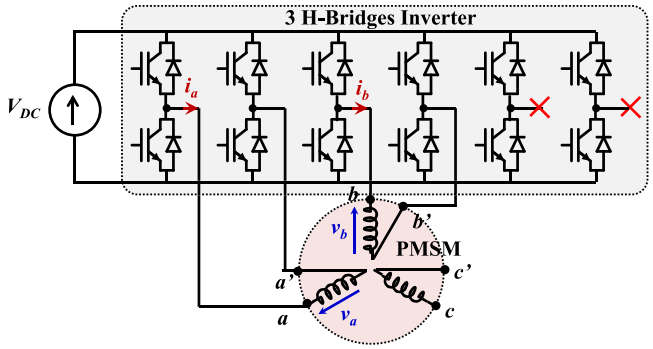

Fig. 4. Fault-tolerant architecture based on a 3 H-bridges inverter.

In the second case, the neutral point voltage is common to each winding leading to a coupling of both phase voltages. As a result the PWM scheme has to rely on a space vector approach [6,15].

3.4. Project framework

The drive requirement is to enable the continuity of service of the traction function when the electric vehicle is on the move. The purpose of the study is to allow the driver to reach an automobile repair shop in order to change the defective devices. This mission can be accomplished at limited speed using a reduced torque range; this option limits any further failure in the motor drive. That is the reason why current range for post fault operation is similar with the one for normal mode. In addition, either in normal mode or in default mode operation, it could be interesting to accurately monitor the dynamic friction in order to adjust the output torque reference [35]; such supervision monitoring system could highly enhance the vehicle speed control at very low speed, which would typically improve drivability during parking operation.

Furthermore the present work focuses on the post fault drive control strategy. It assumes that a robust and effective fault detection and isolation (FDI) technique enables to detect the fault and switch the system to its fault mode. Such technique could be successfully developed by combining the fault tolerant method against current and speed sensor failure [9] and the FDI of phase and switch faults [24].

Finally, the 3-phase motor in default mode operation has been studied and the proposed control scheme defined. The next step is to validate experimentally the advantage of the suggested approach.

4. Innovative approach proof of concept

4.1. Scale and scope of the contribution made

Before addressing the proof of the proposed concept, it seems important to stress the scale and scope of the contribution made in order to place the present work within the context of previous works around similar aspects.

One of the main value of the present proposal is that it offers a comprehensive approach of a multiple input multiple output (MIMO) system based on the physical phenomena occurring in the studied system, namely a 3-phase machine operating only with 2 out of its 3 windings. It hence facilitates understanding and application of the approach by engineers in charge of developing AC motor drives. Significantly, the benefits that electric drive developers may gain from this global approach are numerous in terms of:

- Decoupling between the fictitious control actions (v_γ and v_δ) and (i_γ and i_δ) which enables to design and tune simple PI controllers;
- Torque control which, in steady state, only requires to regulate constant currents. This property is valuable, as it simplifies the current controller's specification: only the torque dynamics response is to consider without taking rotor speed Ω into account. It is therefore easy to meet the drive specifications.

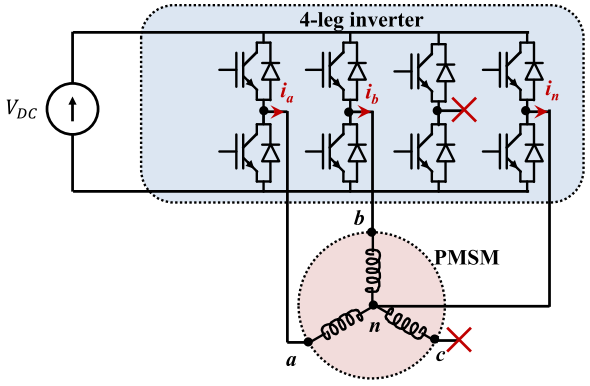

Fig. 5. Fault-tolerant architecture based on a 4-leg inverter.

- Implementation since the developed approach does not make any assumptions except the linearity of magnetics phenomena which principle is commonly accepted regarding motor drive control issues. Consequently, it enables to implement the proposed control structure for any power architecture enabling remedial strategy (see Figs. 4 and 5), namely
    - the 3 H-bridges inverter driving an open-end winding synchronous motor;
    - the 4-leg inverter driving a synchronous motor with a neutral point.

The assets described in the previous paragraph are the simple way to describe the payback that can be achieved from the present contribution. These attractive results are mainly due to the use of two different mathematical transformations (T_i and T_v), one dedicated to the currents, the other one to the voltages. The related model remains convenient to use since the power invariance is fulfilled.

The present proposal was preceded by various works on remedial strategies enabling AC drives to keep working in the event of losing one of the motor winding. The authors were mainly focused on designing dedicated AC machines and power architectures enabling normal and degraded modes operation and on defining the degraded mode current references permitting a constant torque, sometimes considering power losses minimization. The related implementations show that the MIMO system must be controlled differently at the expense of a poorer reference tracking due to disturbance terms, coupling terms or dynamic references.

S. Bolognani et al. [6,7] suggest a control method purely dedicated to a 3-phase machine supplied with a 4-leg inverter. They keep using the classic complete Park transform (abc $\rightarrow$ dqo), which induces to track a sinusoidal zero-current and use an additional inductance in series with the neutral point because of the very small value of the zero sequence inductance.

Mohammad-Ali Shamsi-Nejad et al. [30] and Quntao An et al. [2] addresses the issue of both the power architecture (3 H-bridge inverter versus 4-leg inverter) and current reference waveform optimization. To implement a real-time control, they keep using the partial Park transform (abc $\rightarrow$ dq), which results in some torque fluctuations due to a poor current references tracking. On the other hand, T. Labbé et al. [16] have clearly identified the inappropriateness of using the classic Park transform. They tackle mathematically the control-oriented model issue basing their approach on eigenvectors to diagonalize the machine model. In degraded mode operation, i.e. with two out of three windings operating, the real machine is described by a 2-dimensional equation system: they exhibit properly the two related eigenvectors and eigenvalues, but miss their decoupling goal because applying a single transformation (based on eigenvectors) to both electrical variables, i.e. currents and voltages. Specifically, the mutual inductance M_{ab} induces several harmonic terms which can only be reduced but not canceled by tuning a parameter of the suggested transformation. The simulation of the real-time control reveals significant fluctuations. Baudart et al. [5] address the control issue of a general N-phase machine working with $(N-1)$ windings only in the hypothesis of a specific motor designed with zero coupling effect between the different polyphase-motor windings. It permits the authors to achieve good control and focus on designing the optimal references regarding Joule losses.

According to our best knowledge, although previous research has been extensive, the proposed contribution gives a comprehensive and physics-based approach to address the design of an efficient fault-tolerant control of a 3-phase

Table 2
Leroy Somer LS 132 S synchronous motor parameters.

Symbol	Parameter	Value
R	Stator phase resistance	1.72 (Ω)
L_d	d-axis self-inductance	14 (mH)
L_q	q-axis self-inductance	12.5 (mH)
p	Number of motor pole pairs	4
Ψ_M	Amplitude of the induced flux	0.494 (Wb)
K_{SM}	Back-e.m.f. constant	1.417 (V s)
I	Rated current	10 (A)

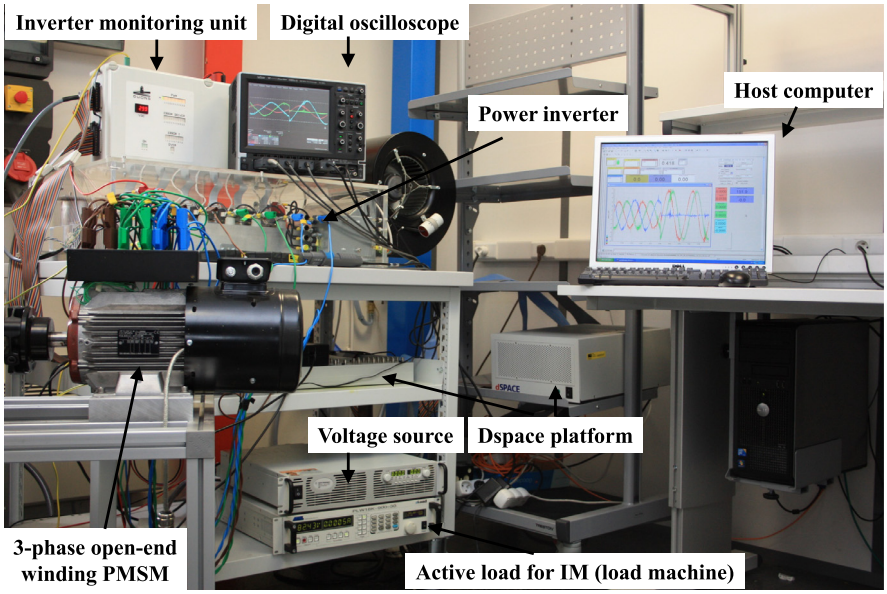

Fig. 6. Experimental setup view.

machine operating in degraded mode operation i.e. using only two out of three windings. Although the theoretical basis is the major contribution, it is also more than important to put into practice the proposed concept for a reality check. That is the goal of the two following sub-sections.

4.2. Experimental test bench

An experimental test bench (Fig. 6) has been developed to validate the innovative control scheme. This enables the drive of the 3-phase machine in the default operation mode. This experimental setup (Fig. 7) is a two part interconnected system.

First, the system under test consists of

- A 3-phase open-end-winding permanent magnet synchronous machine (LEROY SOMER) described in Table 2;
- An incremental encoder (IVO Industry) which provides rotor position data with a resolution of 2500 points per revolution;
- An IGBT inverter made of six legs working at $F_{\mathrm{SW}} = 20$ kHz switching frequency. In the campaign's quantitative research trails, a leg is supposed faulty and hence both legs driving the c winding are inhibited. Only 4 legs work to power the two remaining phases, namely a and b;
- A DC voltage source (AGILENT) supplies the DC bus with 300 V, 11 A rated voltage and current, respectively. It is set to $V_{DC} = 300$ V;
- 2 Hall effect current sensors (LEM) for each motor winding characterized by a high bandwidth (200 kHz) enabling to accurately measure the winding currents;

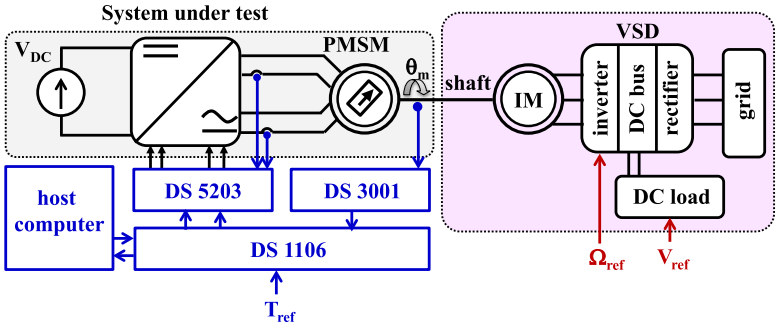

Fig. 7. Control scheme of the synchronous machine in remedial strategy.

A real-time control system is built in a rapid prototyping technology system (designed by DSPACE) around a two-level operating organization. It is organized around a DS1006 processor board ensuring safety and reference management functions as well as the interface between the daughter-boards or the host computer. The DS1006 card is connected with DS 3001 card which permits to give absolute rotor position. It is also interconnected with DS5203 FPGA card equipped with a FPGA Xilinx Virtex® 5 driven with a 100 MHz clock. The latter ensures inverter PWM control signal generation (with a temporal resolution of 10 ns) as well as analog-to-digital conversion (based on a sampling time of 50 μs synchronized with the switching time T_{SW}). All programs are developed using Matlab/Simulink software and then compiled and loaded into the DSPACE system.

As the machine under test is controlled with a torque reference, the second part of the test bench enables the control of the motor shaft rotation speed. It allows the emulation of the load system and hence the mimicking of real application behavior. This second component is composed of:

- A load induction machine (THRIGE ELECTRIC) with two pairs of poles;
- An industrial variable speed drive (OMRON);
- An AC 3-phase electric grid (400 V/50 Hz);
- A voltage-controlled active load (AMREL) with a 600 V voltage reference and connected to the DC stage of the load machine variable speed drive. It allows the recovery of any exceeding power provided by the machine under test.

Using this experimental setup several trials were undertaken and analyzed. They consist of operating the faulty machine in the steady state, the transient state as well as testing the ability of safely switching between healthy and faulty modes.

4.3. Analysis of trial results

4.3.1. Faulty steady state operation mode

To test the control scheme under steady state, the load machine is set at a constant speed, namely 600 r min^{-1}. The current reference is fixed at: $\left[i_{\delta,ref} \quad i_{\gamma,ref}\right]^T = \left[0 \text{ A} \quad 10 \text{ A}\right]^T$. The oscilloscope detects a trigger when the electric angle $\theta_e\,(t)$ passes through π value. Fig. 8 shows the related oscilloscope acquisition. Both real currents i_a and i_b are sinusoidal, have the same magnitude with 60° phase shift and their phase offset regarding $\theta_e = \pi$ are $\pi/6$ and $\pi/2$, respectively. This behavior is consistent with the relationship given in (16). Equally, the current frequency is 40 Hz as expected with a synchronous machine with 4 pole pairs.

4.3.2. Torque transient

In order to assess the torque transient behavior, the second test is an i_γ current step response. The motor shaft is still regulated at 600 r min^{-1} and $i_{\delta,ref}$ is set at zero, whereas a 6.7 Hz pulse generator delivers the i_γ current with two steps at 5 A and 15 A having the same duration. For this high magnitude transient, the time response is small, i.e. about 1.8 ms, and the system signals do not have any overshoot (Fig. 9).

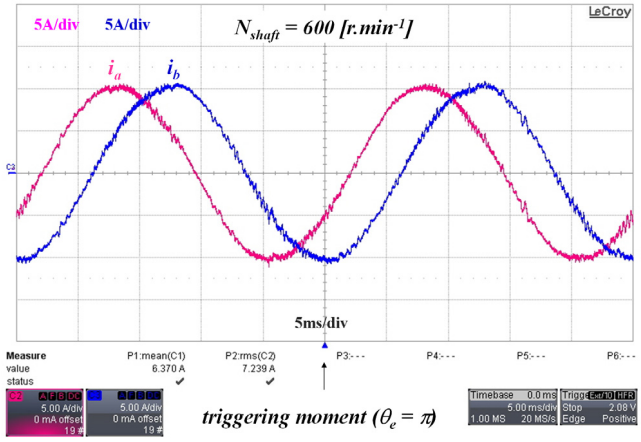

Fig. 8. Stator currents in steady state under fault operation mode: $N = 600$ r min^{-1}, $I_{\delta,ref} = 0$ A and $I_{\gamma,ref} = 10$ A.

4.3.3. Speed transient

The motor current reference is kept constant at $\left[i_{\delta,ref} \quad i_{\gamma,ref}\right]^T = \left[0 \text{ A} \quad 10 \text{ A}\right]^T$ during the third trial period. During this time, the load machine speed reference increases gradually from zero speed to 600 r min^{-1} with a slope of 0.04717 r s^{-2}. The disturbance rejection is completely achieved since the current magnitude is well regulated at 10 A throughout the transient period (Fig. 10).

4.3.4. Switch from healthy to faulty mode operation

Finally it is crucial to assess the ability of the tested architecture to switch safely from a healthy to a faulty operation mode. Several studies have already demonstrated that it is possible to diagnose main faults on such ac drives without adding extra sensors [1,9,24]. For this study it is hence accepted that the inverter or motor default is rapidly detected and isolated. Hence, at $t = 0$ s (i.e. in the middle of the oscilloscope screen) when the c-phase is inhibited in order to simulate an inverter default, it is at the same moment the control scheme switches from the healthy to the faulty algorithm. Despite the fault, the torque reference remains constant at 20 N m. Fig. 11 shows that i_c current falls to zero nearly instantaneously (driven by its own back electromotive force e_c). Meanwhile, both the remaining currents rapidly modify their waveforms. Their phases change and their magnitude increases by a factor $\sqrt{3}$ expanding by 7.1 A to 12.25 A. This test indicates that this architecture provides continuity of service for the driven application. This is a major asset for system reliability and it allows subsequent maintenance to be performed at a convenient place or moment.

5. Conclusion and perspectives

This paper presents a remedial strategy for a fault in a 3-phase synchronous motor. Based on a 4-leg inverter or a 3 independent H-bridge inverter this basic machine is fault-tolerant to a single phase fault, which makes this architecture very attractive. The present work focuses on the appropriate control scheme allowing to address the motor drive in faulty mode operation adequately and efficiently. This is very important since continuity of service is a key factor of modern drives.

The proposed method is based on an innovative voltage and current transformation set which allows not only to decouple the remaining phase dynamics but also to control the electromagnetic torque through constant current references in the steady state. These characteristics make it ideal to use with two independent classic PI controllers. The latter are easy to tune using basic machine parameters. In summary, this approach proposes a general framework for the problem and a solution that is easy to implement.

A proof-of-concept of this theoretical approach has been established on a laboratory test bench using a synchronous machine with 10 A rated current and an IGBT 3-H bridge inverter fed with a 300 V DC voltage

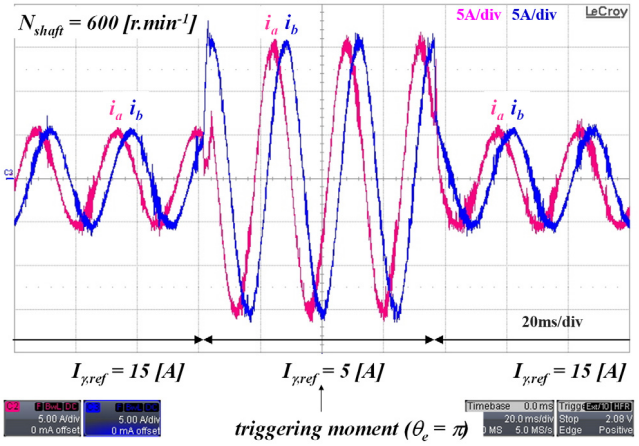

Fig. 9. Stator currents during torque transient under fault operation mode: $N = 600$ r min^{-1}, $I_{\delta,ref} = 0$ A and $I_{\gamma,ref} = 5$ A $\leftrightarrow$ 15 A.

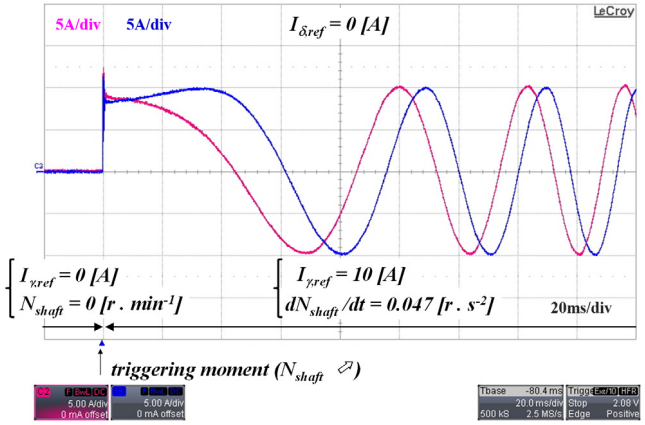

Fig. 10. Stator currents during a speed transient under fault operation mode: $N = 0 \rightarrow 600$ r min^{-1} , $I_{\delta,ref} = 0$ A and $I_{\gamma,ref} = 10$ A .

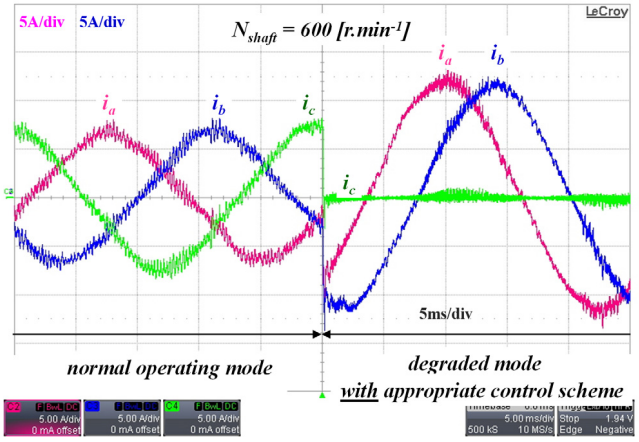

Fig. 11. A fault occurs on c-phase resulting in switching from normal to post-default control scheme: $N = 600$ r min^{-1} and $T_{ref} = 20$ N m.

source. The main motor drive features, namely torque tracking and speed variation, have been successfully validated in degraded operation mode either at steady state or transient state. In addition, in response to a detected default, the switching from healthy to faulty control scheme was successfully tested. In conclusion the experimental results prove that the proposed method gives attractive application prospects in terms of efficiency and simplicity of implementation.

The formulation of the suggested fault-tolerant control strategies is wide-ranging and hence could be extended to induction machine in further work. Another further work perspective is to deal with the implementation of a flux-weakening strategy in the faulty mode operation.

Acknowledgments

The authors gratefully acknowledge the French automotive cluster MOVEO for its financial support through the SOFRACI project (in a FUI program).

References

[1] Qun-Tao An, Li Sun, Li-Zhi Sun, Current residual vector-based open-switch fault diagnosis of inverters in PMSM drive systems, IEEE Trans. Power Electron. 30 (5) (2015) 2814–2827.
[2] Quntao An, Guanglin Wang, Li. Sun, A fault-tolerant operation method of PMSM fed by cascaded two-level inverters, in: 7th International Power Electronics and Motion Control Conference (IPEMC), vol. 2, 2012, pp. 1310–1313.
[3] Sohel Anwar, Wei Niu, Nonlinear observer based analytical redundancy for predictive fault tolerant control of a steer-by-wire system, Asian J. Control 16 (2) (2014) 321–334.
[4] K.J. Astrom, T. Hagglund, PID Controllers: Theory, Design, and Tuning, second ed., Instrument Society of America (ISA), 1995.
[5] F. Baudart, B. Dehez, E. Matagne, D. Telteu-Nedelcu, P. Alexandre, F. Labrique, Torque control strategy of polyphase permanent-magnet synchronous machines with minimal controller reconfiguration under open-circuit fault of one phase, IEEE Trans. Ind. Electron. 59 (6) (2012) 2632–2644.
[6] N. Bianchi, S. Bolognani, M. Zigliotto, M. Zordan, Innovative remedial strategies for inverter faults in ipm synchronous motor drives, IEEE Trans. Energy Convers. 18 (2) (2003) 306–314.
[7] S. Bolognani, M. Zordan, M. Zigliotto, Experimental fault-tolerant control of a pmsm drive, IEEE Trans. Ind. Electron. 47 (5) (2000) 1134–1141.
[8] B. Bouchez, L. De Sousa, Charge transfer device and associated management method, US Patent US20140042807 A1, Feb. 13, 2014.
[9] C. Chakraborty, V. Verma, Speed and current sensor fault detection and isolation technique for induction motor drive using axes transformation, IEEE Trans. Ind. Electron 62 (3) (2015) 1943–1954.
[10] L. De Sousa, B. Bouchez, Combined Electric Device for Powering and Charging, US Patent 20110221363 A1, Sept. 15, 2011.
[11] L. De Sousa, B. Bouchez, Method and Electric Combined Device for Powering and Charging with Compensation Means, US Patent 20120019173 A1, Jan. 26, 2012.
[12] L. De Sousa, B. Bouchez, J.L. Da Costa, Method of exchanging electrical energy between an electrical network conveying a dc or ac electrical quantity and an electrical energy storage unit for hybrid or electric vehicle, European Patent EP2794343 A2, Oct. 29, 2014.
[13] V. M. Hernández-Guzmán, J. Orrante-Sakanassi, Global PID Control of Robot Manipulators Equipped with PMSMs, 20(2) (2018) 1–14.
[14] C.L. Hoo, Sallehuddin Mohamed Haris, Edwin C.Y. Chung, Nik Abdullah Nik Mohamed, New integral antiwindup scheme for pi motor speed control, Asian J. Control 17 (6) (2015) 2115–2132.
[15] A. Kolli, O. Bethoux, A. De Bernardinis, E. Laboure, G. Coquery, Space-vector pwm control synthesis for an H-bridge drive in electric vehicles, IEEE Trans. Veh. Technol. 62 (6) (2013) 2441–2452.
[16] T. Labbé, B. Dehez, F. Labrique, Two phase operation for a three phase PMSM using a control model based on a concordia like transform associated to a classic Park transform, Math. Comput. Simul. 81 (2) (2010) 315–326.
[17] S. Lacroix, E. Labouré, M. Hilairet, An integrated fast battery charger for electric vehicle, in: Proc. VPPC 2010, 2000, Lille, 1–6.
[18] Yongjae Lee, Jung-Ik Ha, Hybrid modulation of dual inverter for open-end permanent magnet synchronous motor, IEEE Trans. Power Electron. 49 (3) (2015) 1256–1263.
[19] P. Lezana, J. Pou, T.A. Meynard, J. Rodriguez, S. Ceballos, F. Richardeau, Survey on fault operation on multilevel inverters, IEEE Trans. Ind. Electron. 57 (7) (2010) 2207–2218.
[20] L. de Lillo, L. Empringham, P.W. Wheeler, S. Khwan-On, C. Gerada, M.N. Othman, Multiphase power converter drive for fault-tolerant machine development in aerospace applications, IEEE Trans. Ind. Electron. 57 (2) (2010) 575–583.
[21] Chee-Shen Lim, E. Levi, M. Jones, N. Abd Rahim, Wooi-Ping Hew, A fault-tolerant two-motor drive with fcs-mp-based flux and torque control, IEEE Trans. Ind. Electron. 61 (12) (2014) 6603–6614.
[22] Faa-Jeng Lin, Shih-Gang Chen, I.-Fan Sun, Adaptive backstepping control of six-phase pmsm using functional link radial basis function network uncertainty observer, Asian J. Control 20 (1) (2018) 1–15.
[23] Faa-Jeng Lin, Ying-Chih Hung, Jia-Ming Chen, Zi-Yin Kao, Sensorless inverter-fed compressor drive system using back-emf estimator with pidnn torque observer, Asian J. Control 16 (4) (2014) 1042–1056.
[24] F. Meinguet, P. Sandulescu, X. Kestelyn, E. Semail, A method for fault detection and isolation based on the processing of multiple diagnostic indices: Application to inverter faults in ac drives, IEEE Trans. Veh. Technol. 62 (3) (2013) 995–1009.

[25] A. Mora, P. Lezana, J. Juliet, Control scheme for an induction motor fed by a cascade multicell converter under internal fault, IEEE Trans. Ind. Electron. 61 (11) (2014) 5948–5955.
[26] M. Naidu, S. Gopalakrishnan, Fault-tolerant permanent magnet motor drive topologies for automotive X-By-wire systems, IEEE Trans. Ind. Appl. 46 (2) (2010) 841–848.
[27] N. Sakr, D. Sadarnac, A. Gascher, A review of on-board integrated chargers for electric vehicles, in: Proc. EPE'14-ECCE Europe, 2014, Lappeenranta, 1-10.
[28] P. Sandulescu, F. Meinguet, X. Kestelyn, E. Semail, A. Bruyere, Control strategies for open-end winding drives operating in the flux-weakening region, IEEE Trans. Power Electron. 29 (9) (2014) 4829–4842.
[29] P. Sekerak, V. Hrabovcova, J. Pyrhonen, S. Kalamen, P. Rafajdus, M. Onufer, Comparison of synchronous motors with different permanent magnet and winding types, IEEE Trans. Magn. 49 (3) (2013) 1256–1263.
[30] M.-A. Shamsi-Nejad, B. Nahid-Mobarakeh, S. Pierfederici, F. Meibody-Tabar, Series architecture for fault tolerant PM drives: Operating modes with one or two DC voltage source(s), in: Industrial Technology (ICIT), 2010 IEEE International Conference on, 2010, pp. 1525–1530.
[31] Y. Song, B. Wang, Survey on reliability of power electronic systems, IEEE Trans. Power Electron. 28 (1) (2013) 591–604.
[32] A. Tani, M. Mengoni, L. Zarri, G. Serra, D. Casadei, Control of multiphase induction motors with an odd number of phases under open-circuit phase faults, IEEE Trans. Power Electron. 27 (2) (2012) 565–577.
[33] M. Villani, M. Tursini, G. Fabri, L. Castellini, High reliability permanent magnet brushless motor drive for aircraft application, IEEE Trans. Ind. Electron. 59 (5) (2012) 591–604.
[34] Z. Wang, J. Chen, M. Cheng, Y. Zheng, Fault-tolerant control of paralleled-voltage-source-inverter-fed PMSM drives, IEEE Trans. Ind. Electron. 62 (8) (2015) 4749–4760.
[35] Xingjian Wang, Shaoping Wang, Output torque tracking control of direct-drive rotary torque motor with dynamic friction compensation, J. Franklin Inst. 352 (11) (2015) 5361–5379.